Title Page:

Dual mechanisms contribute to enhanced voltage dependence of an electric fish potassium channel.

Running title: Electric fish potassium channel.

Jelena Todorovic,[1] Immani Swapna,[1] Antonio Suma,[3] Vincenzo Carnevale,[3] Harold Zakon,[1,2,*]

[1] Dept. of Neuroscience, The University of Texas, Austin, TX 78712, USA

[2] Dept. of Integrative Biology, The University of Texas, Austin, TX 78712, USA

[3] Institute for Computational Molecular Science, College of Science and Technology & Institute for Genomics and Evolutionary Medicine, Temple University. Philadelphia, PA 19122, USA

*Correspondence: h.zakon@austin.utexas.edu

Abstract: The voltage-dependence of different voltage-gated potassium channels, described by the voltage at which half of the channels are open ($V_{1/2}$), varies over a range of 80 mV and is influenced by factors such as the number of positive gating charges and the identity of the hydrophobic amino acids in the channel's voltage-sensor (S4). Here we explore by experimental manipulations and molecular dynamic simulation the contributions of two derived features of an electric fish potassium channel (Kv1.7a) that is among the most voltage-sensitive *shaker* family potassium channels known. These are a patch of four contiguous negatively charged glutamates in the S3-S4 extracellular loop and a glutamate in the S3b helix. We find that these negative charges affect $V_{1/2}$ by separate, complementary mechanisms. In the closed state, the S3-S4 linker negative patch reduces the membrane surface charge biasing the channel to enter the open state while, upon opening, the negative amino acid in the S3b helix faces the second (R2) gating charge of the voltage sensor electrostatically biasing the channel to remain in the open state. This work highlights two evolutionary novelties that illustrate the potential influence of negatively charged amino acids in extracellular loops and adjacent helices to voltage dependence.

Statement of Significance:
The voltage dependence of voltage-gated potassium channels varies considerably. Investigating how potassium channels have evolved such variation in voltage-dependence is important to understanding their function. We studied an electric organ-expressing potassium channel from African weakly electric fish that facilitates the generation of brief action potentials to make a brief electric communication signal. This channel has evolved two mechanisms to enhance its voltage dependence. One is the addition of four consecutive negatively charged amino acids in an extracellular loop that adds to surface charge thereby allowing the channel to open with less depolarization. The other is the addition of a negative charged amino acid near the voltage sensor that holds the channel's voltage sensor in the open position.

INTRODUCTION

The conductance-voltage relationship of voltage-gated channels is typically graphed as a Boltzmann function. The voltage-dependence of a channel is described by the placement of its conductance-voltage (G-V) curve along the voltage axis and the voltage at which half of a population of single channels are open ($V_{1/2}$). Its voltage sensitivity is indicated by the slope of the G-V curve. Voltage-gated potassium (Kv) channels in the *shaker* family (Kv1-4) show a wide range of voltage-dependences from those that activate at highly depolarized membrane potentials ($V_{1/2}$ = +33 mV: jshak1, a jellyfish channel), (1) to those that activate close to resting potential ($V_{1/2}$ = -50 mV: Kv4.1; jShal1 = -39mV) (2,3). These differences in voltage dependence are critical for the roles specific Kv channels play in shaping neuronal activity, but also offer an entrée into the structure-function relationship of Kv channels.

Among the Kv channels that activate at the most hyperpolarized potentials are Kv1.7a of mormyrid electric fish from Africa ($V_{1/2}$ = -44 mV: Kv1.7a *Brienomyrus brachyistius*; $V_{1/2}$ = -52 mV: Kv1.7a, *Campylomormyrus compressirostris*) (4). Kv1.7 is expressed in muscle in vertebrates (5,6). As a result of a whole genome duplication at the origin of teleosts, the gene encoding Kv1.7 duplicated into two paralogs in fish (the gene kcna7a encodes the Kv1.7a channel and the kcna7b gene encodes the Kv1.7b channel). In a relative of the mormyrids, *Gymnarchus niloticus*, the kcna7a gene still expresses in muscle whereas during the evolution of the electric organ, mormyrids lost kcna7a expression in muscle and gained it in the electric organ where it underwent a burst of positive selection (4). Many mormyrids make extremely brief electric organ discharges (7,8) based on brief (~200 μsec) action potentials from their electric organ cells (9,10). The enhanced voltage-sensitivity of the mormyrid Kv1.7a helps shorten the electric organ action potential duration (4).

A channel's voltage-dependence and voltage-sensitivity are influenced by the number of positive charges in its voltage sensor (S4 helix) (11) and the identity of the hydrophobic amino acids between them as pioneered by the Aldrich lab (12,13) and others (14,15). Less well studied is the role of charged amino acids in some of the extracellular loops that influence a channel's voltage-dependence by altering membrane surface charge (16-19). A small region of an extracellular loop--the S3-S4 linker-- is critical for the difference in $V_{1/2}$ between Kv1.7a of *Brienomyrus* and *Gymnarchus* in which kcna7a is still expressed in the muscle ($V_{1/2}$ = -13 mV). This region of the S3-S4 linker is composed of neutral amino acids in most Kv channels, as it is in *Gymnarchus*. However, in the homologous region the Kv1.7a of mormyrids possesses an evolutionarily derived feature, a cluster of three or four negatively charged glutamates (E) (Fig. 1). Transfer of the four glutamates in the "negative patch" from *Brienomyrus* to *Gymnarchus* largely confers the $V_{1/2}$ of *Brienomyrus* onto the *Gymnarchus* channel, and *vice versa*. It is likely that the negative patch influences channel properties by its effect on the membrane surface charge (4). Additionally, mormryid Kv1.7a channels have another derived amino acid substitution: a negatively charged amino acid in the S3b helix (Fig. 1). Charge substitution at this site (E>K) right-shifts $V_{1/2}$ by +25 mV suggesting that this site also plays a role in channel voltage-dependence (4).

Here we use site-directed mutagenesis and molecular dynamic (MD) simulations to assess the roles of negative charges at these two sites in influencing $V_{1/2}$. We found that these two sites influence voltage-dependence by different but complementary mechanisms: the negative patch in the S3-S4 linker contributes to surface charge allowing the channel to open at more hyperpolarized membrane potentials, and the negative amino acid in the S3b acts as a novel countercharge to the second (R2) gating charge in the S4 voltage sensor holding the channel in the open state.

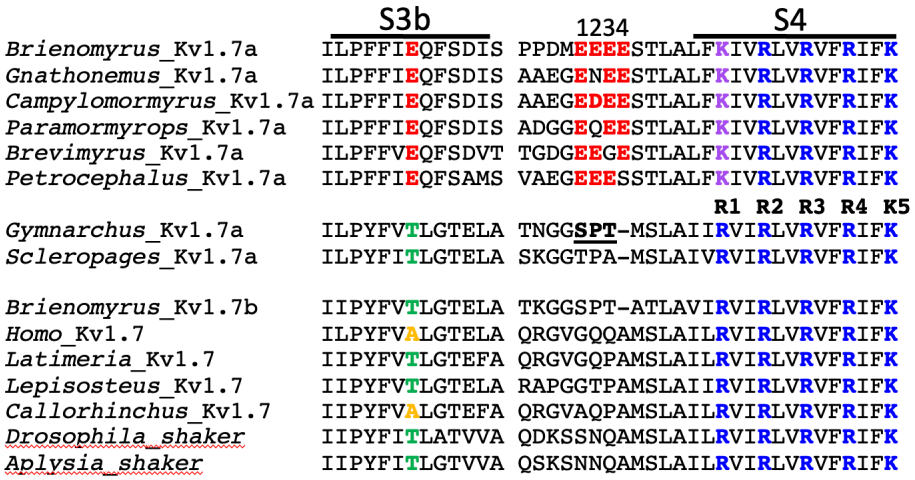

Figure 1—Amino acid (AA) sequence of *shaker* family channels illustrating the position of the negatively charged glutamate in the S3b helix (E299) and the "negative patch" in the S3-S4 loop (numbered 1-4 corresponding to E311-E314) of mormyrid electric fish (red = negative AAs; blue = positive gating charges in S4 labeled R1-K5; purple = mormyrid-specific lysine at position R1; green, orange = neutral AAs). *Brienomyrus brachyistius*, *Gnathonemus petersii*, *Campylomormyrus compressirostris*, *Paramormyrops kingsleyae*, *Brevimyrus niger*, and *Petrocephalus soudanensis* are all mormyrids in which Kv1.7a is expressed in the electric organ and which have these two derived features. *Gymnarchus niloticus* is an electric fish related to mormyrids; its Kv1.7a is expressed in muscle with an S3b with T298 (orthologous position to E299) and S3-S4 composed of neutral AAs as in the other Kv channels illustrated here. The three AAs from *Gymnotus* Kv1.7a that were experimentally swapped for the negative patch in chimeric channels are bolded and underlined. *Scleropages formosus* (Asian arowana), is a non-electric relative of mormyrids. Also shown is the Kv1.7b of *Brienomyrus*, the paralog of Kv1.7b expressed in muscle. Shown for comparison are the Kv1.7 of *Homo sapiens* (humans), *Latimeria chalumnae* (Coelacanth), a close tetrapod relative, *Lepisosteus oculatus* (spotted garfish), a close teleost relative, *Callorhinchus milli* (elephant shark), an elasmobranch, and the *shaker* channels of *Drosophila melanogaster* (fruit fly), and *Aplysia Californica* (California sea hare).

MATERIALS AND METHODS

Xenopus laevis oocyte isolation

Frogs were purchased from Nasco, (Fort Atkinson, WI, USA), and housed at the animal resource center at the University of Texas, Austin. When needed, oocytes were surgically removed in accordance with the National Institutes of Health guidelines for the care and use of laboratory animals. The *Xenopus laevis* surgery was performed using tricaine anesthesia, described in the protocol that was reviewed and approved by IACUC of the University of Texas at Austin. After removal, oocytes were kept in isolation media (in mM: 108 NaCl, 10 HEPES, 2 KCl and 1 EDTA), which causes a slight dehydration of the oocyte, allowing for easier manual removal of the thecal and epithelial membrane layers. This was then followed with a removal of the follicular layers using collagenase solution (mM: 83 NaCl, 5 HEPES and 2 MgCl2 with 5 mg/10ml collagenase D enzyme). To accomplish this step, oocytes were left in the collagenase solution for 10 min, washed with clean modified Barth's solution, and then transferred into clean, sterile MBS until ready to be injected with mRNA, using the micro injector from Drummond Scientific Co. (Broomall, PA, USA). After injections were completed, oocytes were divided and kept individually in sterile 96 well plates

(Corning Costar flat bottom, or similar) in incubation media (MBS enriched with 2mM Na pyruvate, 0.5 mM theophylline, 10 U/ml penicillin, 10 mg/l streptomycin and 30 mg gentamycin, with the entire solution sterilized by filtration using 0.22 mm filter). Plates were then kept in dark, at 16^{o}C until ready for experiments.

Site-directed mutagenesis, mRNA synthesis and kcna7a protein expression

Brienomyrus brachystius (MH137731.1) and *Gymnarchus niloticus* (MH137725) kcna7a coding sequences were synthesized by GenScript (Piscataway, NJ, USA). They were cloned into the pGEMHE vector, with the Kozak sequence (GCCACC) added to the 5' end, ahead of the start codon to increase translation. Mutations were then introduced using the QuickChange II XL site directed mutagenesis kit from Agilent (Santa Clara, USA) which was followed by sequencing to check for accuracy of the cDNA construct. Once the cDNA sequences were confirmed, *in vitro* transcription was performed using mMESSAGE mMACHINE T7 Transcription Kit (Thermo Fisher Scientific, USA), following the manufacturers protocol. After getting the mRNA concentrations using the ND-1000 spectrophotometer from NanoDrop Technologies, (Wilmington, DE, USA), *Xenopus laevis* oocytes were isolated and prepared, as described above, and injected with 50 nl of 0.01–0.1 µg/µl mRNA (suspended in nuclease free water). Plates were kept in the dark, at 16^{o}C until ready for experiments (usually between 1-4 days).

Electrophysiology and analysis

Currents were recorded at room temperature (21-23^{o}C), using the two-electrode voltage clamp (OocyteClamp OC 725C amplifier from Warner Instruments Corp, Hamden, CT, USA). During most of the recordings the main bath solution contained, in mM: 115 NaCl, 1.5 KCl, 10 HEPES and 1 MgCl2, pH adjusted to 7.4 with NaOH, and the pipette solution consisted of 3 M KOAc and 15 mM KCl. The bath solution deviated from this recipe only during the strontium and urea experiments. Current activation was measured using a series of 10 mV steps of 100 ms duration each. These steps were taken from a potential of -90 mV to 40 mV, followed by a 100 ms pulse of -50 mV. For currents from *Brienomyrus brachystius* mutants that were opening at a more depolarized potentials the voltage steps were adjusted to -70 to 60 or 80 mV in 10 mV increments. The K^+ reversal potential was calculated by a pulse protocol of 100 ms depolarization steps to 40 or 60 mV followed by a 200 ms test pulse of -120 mV to 0 mV in 10 mV increments. In all experiments, the holding potential was -90 mV. Recordings were made for each experimental condition from at least three independently collected batches of oocytes to minimize any potential batch effects.

pCLAMP 11 software from Axon instruments Inc. (Foster City, CA, USA) was used for preliminary analysis and acquisition of raw I-V data. The rest of the analysis was done using the GraphPad Prism 9. (Boston, USA). The ionic current (I) recorded during the voltage steps was converted to conductance (G) by dividing with the driving force ($V-E_{rev}$). The half-activation potential ($V_{1/2}$) and slope factor of the activation curve were obtained by fitting the G-V curves with a simple Boltzmann function. Unless otherwise specified, comparisons of experimental groups were made with a one-way ANOVA, with post hoc Dunnett's test. Measures of variation are given as standard error of the mean (SEM).

Molecular Dynamics Simulation

We generated the initial structural models using an homology modelling protocol based on the NavAb structures obtained via Cryo-EM described in refs. (20,21). The sequence alignment between the templates and the *Brienomyrus* Kv1.7a and *Gymnarchus* Kv1.7a genes is taken from ref. (22).

Threading of sequences into the template structures was carried out using the SWISS-MODEL webserver (23). To refine loops and unstructured regions, we used Rosetta *Kinematic closure* (24) and an *ab initio* loop structure prediction protocol based on the Rosetta membrane score function (25). For each linker, we generated about 5000 models, and clustered them based on their root mean square deviations,

using the Jarvis-Patrick methods implemented on the software GROMACS [https://doi.org/10.1016/j.softx.2015.06.001]. For clustering, we used a cutoff of 0.8nm, and a minimum number of neighbors equal to 4. We then selected the most representative model of the largest cluster.

Molecular systems were initialized using the CHARMM-GUI webserver (26) . We embedded the membrane proteins in a lipid bilayer of POPC and solvated the system in a KCl solution with a concentration of 0.15 M (potassium ions were the only cations present in solution).

Each system consists of about 200000 atoms in total. Calculations are performed using the NAMD2 computational code (27), using the all-atom potential energy function CHARMM36 for protein and phospholipids, and the TIP3P potential for water molecules (28)].

Periodic boundaries conditions are applied, and long-range electrostatic interactions are treated by the particle mesh Ewald algorithm (29). Molecular systems are equilibrated for about 3 ns with decreasing harmonic restraints applied to the protein atoms, the pore ions, and the water molecules localized in the filter. All trajectories are generated with a time step of 2 fs at constant normal pressure (1 atm) controlled by a Langevin piston and constant temperature (300 K) using a Nosé-Hoover thermostat. The simulations were run for about 200ns for each model.

RESULTS

Strontium shifts $V_{1/2}$

One way to assess the role of negatively-charged amino acids in extracellular loops on a channel's voltage-dependence is to temporarily remove their electrical influence by screening them with divalent cations--historically Ca^{2+} (30,31) but nowadays usually Mg^{2+} , Sr^{2+},or Ln^{3+}--in the extracellular bathing solution (16,32,33). While this method does not target specific amino acids, it can be used to great effect in combination with amino acid substitutions or swapping small regions across different channels (18).

We compared the properties of expressed wild type Kv1.7a channels from *Brienomyrus* and *Gymnarchus* and chimeric channels with reciprocal swaps of a portion of the S3-S4 linker (EEEE from *Brienomyrus* and SPT from *Gymnarchus*) region when perfused with saline, urea (120 mM: as a control for osmolarity following (18) and due to its low membrane permeability in *Xenopus* oocytes (34)), or $SrCl_2$ (50 mM) (Fig. 2). Urea had little or no effect on channel properties indicating that none of the effects described below are due to changes in osmolarity of the extracellular solution.

Perfusion of *Gymnarchus* Kv1.7a with $SrCl_2$ shifted the G-V curve only slightly rightward ($p<0.05$). The SPT>EEEE chimeric channel had a significantly left-shifted G-V curve ($p< 0.001$) and application of $SrCl_2$ to this chimeric channel shifted the G-V curve rightward virtually superimposing it on the other two G-V curves (WT Gn vs. GnSPT>EEEE, p= N.S.; WT Gn/$SrCl_2$ vs. Gn SPT>EEEE/$SrCl_2$, p = 0.05) (Fig. 2A). These results imply that the *Gymnarchus* Kv1.7a has few electrostatically important negative charges in its extracellular loops. They also demonstrate that $SrCl_2$ can almost completely screen the introduced negative charge in the SPT>EEEE chimeric channel.

As we previously demonstrated, removal of the negative patch in the *Brienomyrus* chimeric channel [EEEE>SPT] altered voltage-dependence significantly shifting the G-V curve rightward. Perfusion of wild type *Brienomyrus* Kv1.7a with $SrCl_2$ shifted the G-V curve rightward the same amount as removal of the negative patch in the EEEE>SPT chimeric channel (WT Bb/$SrCl_2$ vs. Bb EEE>SPT, p = N.S.) (Fig. 2B). In fact, there was no significant difference between WT Bb/$SrCl_2$ and WT Gn, or GnSPT>EEEE/$SrCl_2$. This, again, suggests that the negative patch supplies most of the accessible negative charges (Fig. 2C). Application of $SrCl_2$ to the EEEE>SPT chimeric channel moved $V_{1/2}$ even further rightward (WT Bb vs. Bb EEEE>SPT/$SrCl_2$, p = 0.001), which was unexpected considering the other results so far from both channels.

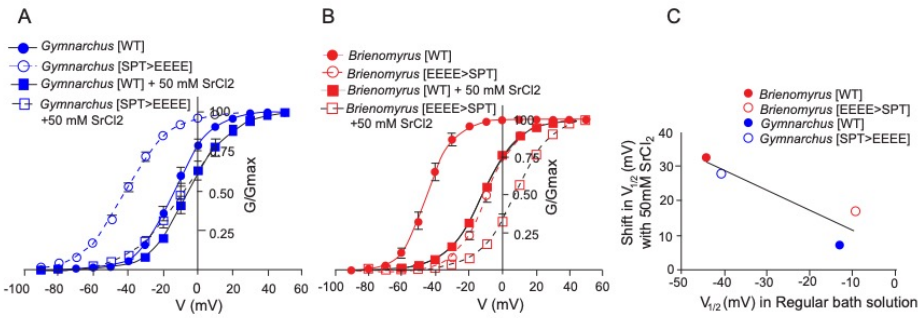

Figure 2—Strontium right-shifts G-V curves. (A) Relationship between the shift of $V_{1/2}$ in $SrCl_2$ versus baseline $V_{1/2}$ in wild type channels [WT] *Gymnarchus* Kv1.7a channels or those in which the negative patch in the S3-S4 linker from *Brienomyrus* replaced the homologous region from *Gymnarchus* [SPT>EEEE] (B) Same experimental conditions using Kv1.7a from *Brienomyrus* with the S3-S4 linker substituted with that of *Gymnarchus* [EEEE>SPT]. The extent of shift is related to the presence of the negative patch. (C) Correlation between shift of $V_{1/2}$ after $SrCl_2$ treatment vs. baseline $V_{1/2}$. R = 0.81. Error bars = S.E.M.

Number and Location of Negative Charges in S3-S4 Linker Influence $V_{1/2}$

In our previous study (4), we manipulated all four glutamates together. We wondered if all or only some of the glutamates (numbered according to their position in the linker as: 1 = E311, 2 = E312, 3 = E313, 4 = E314; Fig. 1) —for example, only those closest to S4—affect $V_{1/2}$. We assessed the impact of the number and locations of the glutamates in the S3-S4 linker on $V_{1/2}$ by substituting glycines or serines in their place following Sand et al. (2013). In our previous study we removed all four glutamates, and replaced them with three different amino acids from *Gymnarchus* (SPT). Here, for consistency, we used only a single species of amino acid at a time for replacement and replaced with the same number that we removed.

First, we substituted pairs of either glycine or serine for the odd or even numbered glutamates (even: EGEG, ESES; odd: GEGE, SESE). We noted that glutamates in the second and fourth positions in a background of glycines are more effective in moving $V_{1/2}$ toward negative potentials than glutamates in the first and third position ($p < 0.007$) (Fig. 3). There was a slight, but non-significant, position effect in the same direction in a background of serines. There was no significant difference between replacing the background amino acids with glycine or serine in similar placements (EGEG = ESES or GEGE = SESE).

Next, we tested the location of a single glutamate in each of the four positions and since there was little difference in serine or glycine as replacements in the previous experiment we only replaced with glycine (EGGG, GEGG, GGEG, GGGE). There was no significant difference among these values indicating that a glutamate at any location within the negative patch can affect $V_{1/2}$ ($p = 0.14$) (Fig. 3). We tested these data against a control condition of four glycines (GGGG). This was significantly different from the previous dataset ($p<0.0001$) demonstrating that the presence of even a single glutamate significantly shifts $V_{1/2}$. Finally, the $V_{1/2}$ for the GGGG (-7.4 ± 2.0 mV) is not statistically different ($p= 0.4$) from the $V_{1/2}$ for *Brienomyrus* with the *Gymnarchus* S3-S4 linker (SPT) substituted for the four glutamates (-9.4 ± 1.4 mV) proving that glycine is a suitable amino acid for replacing the glutamates in the background of the *Brienomyrus* channel and that the difference in the number of replaced amino acids (three vs. four) does not matter. Taking the difference between the $V_{1/2}$ of the GGGG construct and the average of the $V_{1/2}$ of the four constructs with a single glutamate (EGGG, GEGG, etc.) shows that, on average, a single glutamate contributes ~-13.5 mV to the $V_{1/2}$ of the *Brienomyrus* Kv1.7a channel. If the effect of the glutamates on $V_{1/2}$ added linearly, they should contribute -54 mV to $V_{1/2}$ whereas they contribute only -35 mV (difference

in $V_{1/2}$ between WT and EEEE>SPT) suggesting that they add sub-linearly. This shows that while the contribution of each glutamate to $V_{1/2}$ is substantial, they add with diminishing returns.

We explored possible reasons for the negative charges to add sub-linearly. The presence of multiple neighboring titratable groups affects their dissociation equilibrium, raising the possibility that only a fraction of them are protonated at each moment in time. To explore this possibility, we used PropKa (35) to predict the pKa of E311, E312, E313, and E314. Results indicate that all the side chain carboxylic acids are dissociated (and thus negatively charged) in both the resting and activated state. Indeed, all the pKa values are significantly lower that the neutral pH value of 7: they are 4.4, 4.5, 3.6, and 4.1 in the activated state and 4, 4.5, 4.3, and 4.9 in the resting state for E311, E312, E313, and E314, respectively.

The slopes of the G-V curves did not differ across groups ($p< 0.11$) supporting the idea that the "negative patch" only affects surface charge but does not interact with the voltage sensor (Fig. 4).

These results in combination with MD simulations (below) reinforce our conclusion (4) that specific glutamates in the S3-S4 linker do not interact with other amino acids in the channel *via* salt bridges but, rather, in the aggregate, add to surface charge.

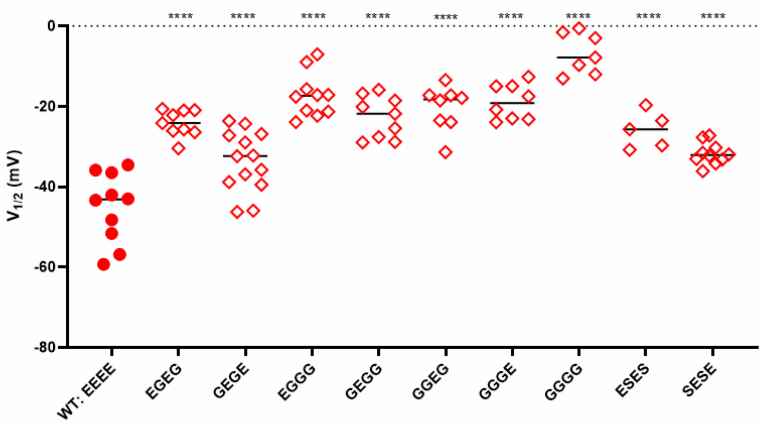

Figure 3—Substitution of neutral amino acids glycine (G) or serine (S) into the negative patch of *Brienomyrus* Kv1.7a (WT: EEEE) shift $V_{1/2}$ to more positive values. The position and number of substitutions is given on the x axis. Black horizontal line = mean. Filled circles = WT (wild type) and open diamonds = glutamate substitutions. All groups are significantly different ($p< 0.001$) from WT.

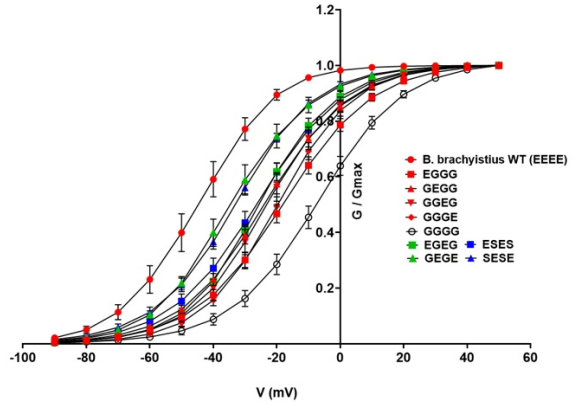

Figure 4—Decreasing the numbers of glutamates in the negative patch right-shifts the G-V curve but does not affect their slopes. Error bars = S.E.M.

Amino Acid Substitutions in S3b of *Brienomyrus* Kv1.7a Alter $V_{1/2}$

The presence of E299 in the Kv1.7a channel from six species spanning mormyrid phylogeny (Fig. 1) suggests that a glutamate substitution occurred in a mormyrid ancestor. Alignments of *shaker* subfamily channels from a broad sampling of animals show that a threonine at this site is highly conserved. The only exception in vertebrates is the independent substitution of an alanine in Kv1.7 of tetrapods and shark (Fig. 1).

At the codon level, a threonine-to-glutamate substitution calls for a dinucleotide change. The most parsimonious series of substitutions is from threonine (ACA or ACG), to alanine (GCA or GCG), to glutamate (GAA or GAG). We investigated the consequences of alanine and glutamate substitutions in *Gymnarchus* Kv1.7a as a proxy to estimate how channel properties might have been affected during the evolutionary transitions at this site in mormyrids. Alanine and glutamate substitutions in *Gymnarchus* had little to no effect on $V_{1/2}$ (Fig 5A). We then tested the sensitivity of this site to a range of AAs. Substitution of the polar AAs glutamine and asparagine had no effect on $V_{1/2}$. Negatively charged aspartate slightly but significantly shifted the $V_{1/2}$ in a more depolarized direction (~+5 mV). The polar, hydrophilic, and positively charged AAs lysine and arginine significantly elevated $V_{1/2}$ by ~+15 mV. Conversely, the substitution of hydrophobic AAs (leucine and isoleucine) strongly moved $V_{1/2}$ to more negative values (~-25mV). Thus, despite strong conservation of threonine at this site in animal *shaker* subfamily channels, negatively charged or polar AAs had little effect on $V_{1/2}$.

Brienomyrus Kv1.7a was more sensitive to AA substitutions at this site (Fig 5B). The glutamate-to-alanine or threonine substitutions in *Brienomyrus* raised $V_{1/2}$ by ~+10 mV suggesting that in the context of the complete set of evolutionary changes in the ancestral mormyrid channel, a glutamate at this site is important to confer enhanced voltage-sensitivity. Substitution of other polar AAs, even the negatively charged aspartate, similarly reduced voltage dependence. In agreement with *Gymnarchus* Kv1.7a, substitution of positively charged AAs raised $V_{1/2}$ ~+20 mV and substitution of hydrophobic leucine lowered it by ~-20mV. None of the substitutions in Kv1.7a of either species affected the slope factor except for the strongly hydrophobic ones (Isoleucine and leucine) (Figs. S1-S3).

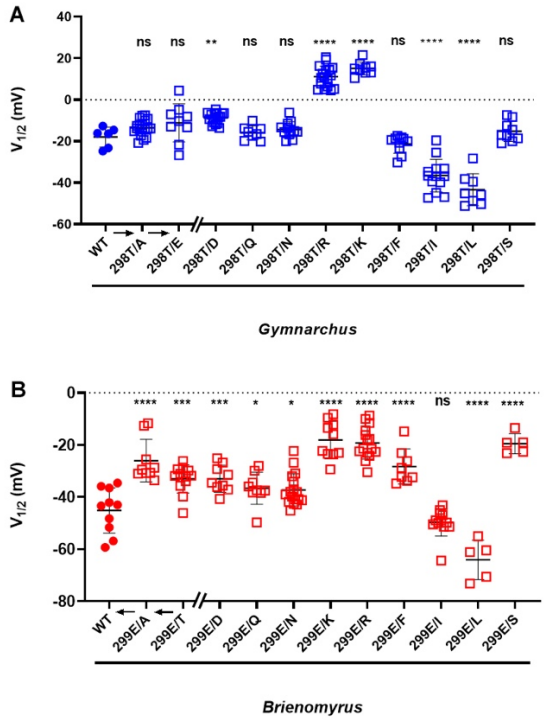

Figure 5—Amino acid substitutions at the orthologous site in *Gymnarchus* (T298) (A) and *Brienomyrus* (E299) (B) alter $V_{1/2}$. Arrows along x axis indicate the likely evolutionary transition T>A>E for site 299 in *Brienomyrus* S3b. Arrows along x axis for *Gymnarchus* show how a similar transition would have little impact on $V_{1/2}$ in a *Gymnarchus* background. All comparisons are made between WT and experimental groups.

Because the $V_{1/2}$ of *Drosophila Shaker* is strongly influenced by the aggregate hydrophobicity of S3b, (36) we assessed the effect of hydropathy at this site and observed that $V_{1/2}$ is significantly related to hydropathy in *Gymnarchus* when all amino acids (r = -0.79; N = 12; p = 0.0018) or even only uncharged amino acids (r = -0.73; N = 8; p = .038) are tested (Fig. 6A,B). There is no significant correlation in *Brienomyrus* whether all (r = -0.49; N = 12; p = NS) or only uncharged amino acids are tested (r = -0.43; N =8; p = NS) (Fig. 6C,D). Thus, while this relationship in *Gymnarchus* is predicted by results from *Drosophila* (36), additional factors are involved in setting the $V_{1/2}$ of the *Brienomyrus* channel.

In sum, *Gymnarchus* Kv1.7a is robust to substitutions of biochemically similar AAs whereas substitutions in *Brienomyrus*, even of a highly similar AA (glutamate>aspartate) generally reduce voltage dependence demonstrating that a glutamate at this site is functionally critical for *Brienomyrus* Kv1.7a. However, both channels become less voltage-dependent with positive residues at this site, and more voltage-dependent with some hydrophobic residues.

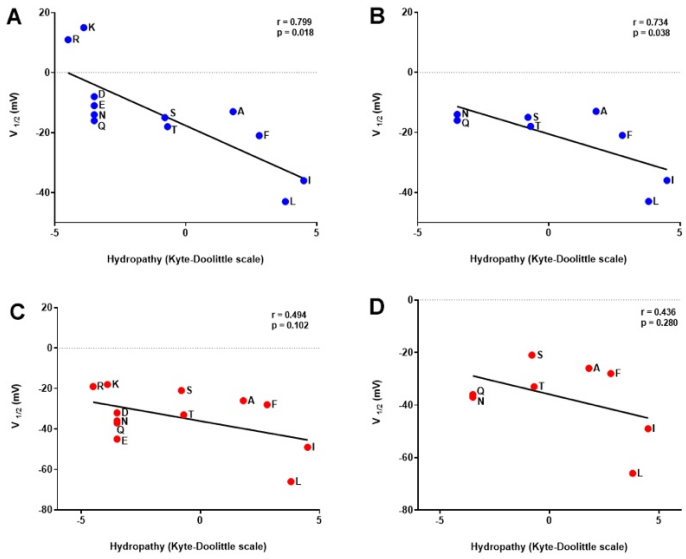

Figure 6—Relationship between $V_{1/2}$ and hydropathy at orthologous site E299/T298. (A) All substitutions at T298 in *Gymnarchus;* (B) same data as in A but with charged amino acids removed. (C) All substitutions at E299 in *Brienomyrus;* (D) same data as in C but with charged amino acids removed.

Molecular Dynamics Simulations Support "negative patch" Surface Charges and Identify E299 as a Novel Countercharge.

We performed all atom simulations of *Brienomyrus* Kv1.7a and *Gymnarcus* Kv1.7a, both in the resting and activated state (see methods for setup details). Figure 7 shows the equilibrated conformations after about 200 ns of MD simulations.

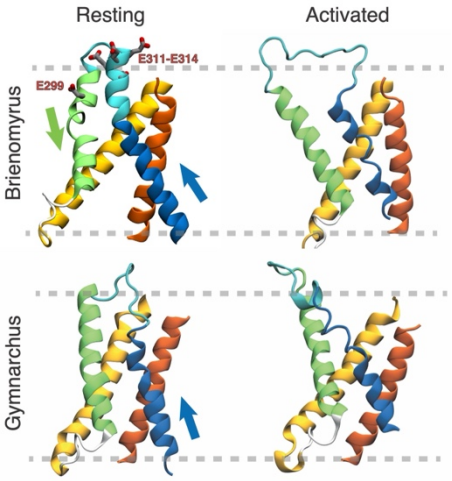

Figure 7--Equilibrated structures of *Brienomyrus* Kv1.7a and *Gymnarchus* Kv1.7a in the resting and activated states. The dashed lines indicate the position of the lipid bilayer headgroups, while the arrows indicate the downward and upward movements that the S3 and S4 helices undergo on passing from the resting to the activated state. In the top-left panel, we highlighted the S3b charge (E399) and the linker surface charges (E311-E314). The coloring scheme of the proteins is the following: S1-orange, S2-yellow, S3-green, S3-S4 linker-light blue, S4-blue. PDB files are in the supplement.

A key observation is that, in the resting state of *Brienomyrus* Kv1.7a, a continuous helix (in cyan in Fig. 7) is observed from E311 to F320 encompassing both the negative patch from the S3-S4 linker and S4. This secondary structure element shows persistent conformational stability over 200 ns. As a result, the negatively charged amino acids E311--E314 rather than being solvent exposed are located well within the low dielectric region of the lipid bilayer. By contrast, the S3-S4 linker of *Gymnarchus* Kv1.7a does not show any secondary structure content.

An interesting and unique feature of the resting state of *Brienomyrus* Kv1.7a is the interaction of the E311-E314 negative charge cluster with cations from the extracellular medium or positively charge moieties from the lipid head groups (Fig. 8). Importantly, cations might be chelated by more than one carboxylate and thus establish "salt-bridges" between different parts of the channel as, for instance, in the case of E311 and D379. Surprisingly, these glutamates do not make actual salt bridges with any positively charged amino acid. In the activated state, the negative cluster is surrounded only by mobile cations and lipid head groups and does not coordinate cations together with other negative amino acids (Fig. 8).

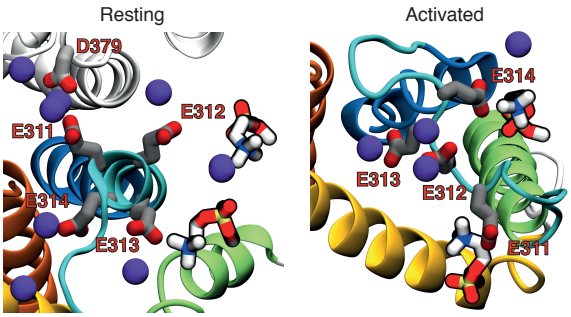

Figure 8--Top view of *Brienomyrus* Kv1.7a in the resting and activated states. Highlighted are E311, E312, E313, E314, the potassium ions from solution (blue) that are within 10 Å from any of these negatively charged amino acids, and the positive moieties from the lipid (carbon backbones are white) head groups that interact with the negative cluster. In the resting state, residue D379 is highlighted, as it coordinates two cations together with E311. The coloring scheme for the proteins is in Fig. 7.

For both *Brienomyrus* Kv1.7a and *Gymnarchus* Kv1.7a an accumulation of cations is observed on the extracellular side of the lipid membrane. However, the excess of positive charge with respect to the bulk is much more pronounced in *Brienomyrus* Kv1.7a (Fig. 9). Importantly, this peak in the density of cations occurs in the interfacial region of the membrane where the lipid head groups are located (Fig. 10). In the activated state, the ion density is still peaked around the position of the negative cluster *Brienomyrus* Kv1.7a, while it is completely flat in *Gymnarchus* Kv1.7a (Fig. 9). Thus, the modeling confirms the role of the negative patch in neutralizing positive charges that reside in or near the membrane.

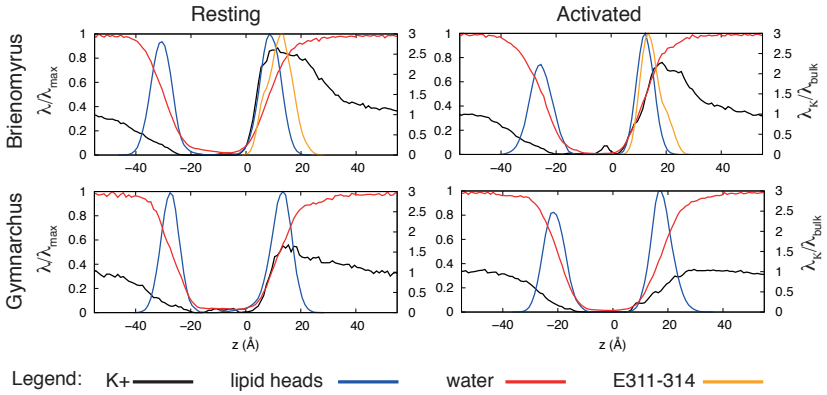

Figure 9--Number density of potassium ions (black), lipid head-groups (blue), waters (red) and negative patch (orange). The number density of potassium ions λ_K is rescaled by its bulk value (y-values on the right), while the other three densities are rescaled by their peak values λ_{max} (y-values on the left).

On passing from the resting to the activated state, S4 moves upward with respect to the membrane plane as described in many other studies (37,38). The S3 helix movement is accompanied by a rotation of a key residue, E299, in *Brienomyrus* Kv1.7a. While in the resting state E299 faces the lipid membrane, and interacts with it, in the activated state it rotates by ~75° and faces the lumen of the voltage sensor domain where it interacts with R324 (Fig. 10), as highlighted by an average distance of about 1.5 Å. Importantly, bidentate binding with two simultaneous hydrogen bonds is possible, given the orientation of the R324 guanidinium group. Moreover, in the activated state we do see additional binding interactions with D238, and less probably with D303, E311 and E216. Overall, they all contribute to stabilizing this state. For this reason, even though the E299D mutation produces a leftward shift in the G-V curve of about 10 mV, we did not observe major structural differences or changes in the interaction geometry upon mutation, likely because all these additional charged amino acids contribute to stabilize the structure.

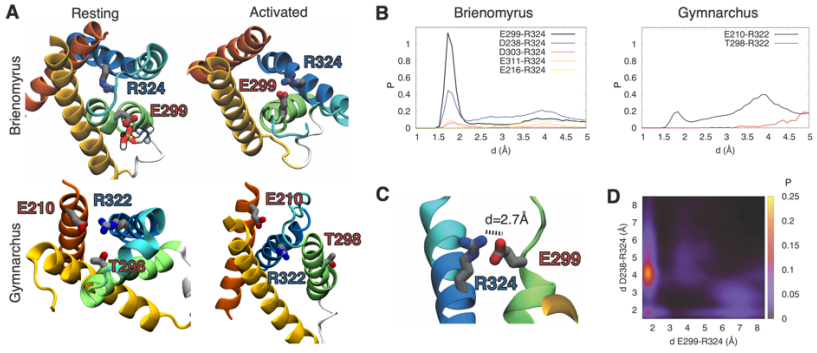

Figure 10--A. Top view of *Brienomyrus* Kv1.7a and *Gymnarchus* Kv1.7a in the resting and activated states. (A) In *Brienomyrus* Kv1.7a, E299 faces the lipid membrane in the resting state, while it interacts with R324 in the activated state (see panel C). B. Left panel: the distribution of the minimum distance between all charged amino acids found to have a distance of less than 2Å from the second gating charge R324 in the activated state. The first and second most frequently bound amino acids are E299 and D238, see also 2D histogram in panel D. Right panel: same distribution as in left panel calculated for *Gymnarchus* Kv1.7a.

Only E210 is found to bind to the second gating charge R322, but not as frequently or tightly as E299. Also plotted is the distribution distance between T298 (corresponding to E299 of *Brienomyrus*) and R322. The latter amino acid undergoes a similar rotation, however no interaction is observed between T298 and R322. The coloring scheme for the proteins is in Fig. 7. Panel C: zoom in on the E299-R324 interaction in the activation. Panel D: two dimensional histogram of D238-R324 vs E299-R324 distances.

For *Gymnarchus* Kv1.7a, the amino acid corresponding to E299, namely T298, undergoes a similar rotation between the membrane-facing conformation in the resting state, and the lumen-facing one in the activated state (Fig. 10). However, T298 is not sufficiently extended or charged to interact with the gating charge R322 (corresponding to R324 in *Brienomyrus* Kv1.7a). In this case, the average distance is about 6 Å. Moreover, in this case we found that only E210 can interact with R322, although with much lower frequency.

Deactivation of Kv1.7a Supports Interaction of *Brienomyrus* E299 with R324

Voltage clamped Kv1.7a currents from *Brienomyrus* (and another mormyrid, *Campylomormyrus*, fig. 1) deactivate significantly more slowly than those of *Gymnarchus* (4). We reasoned that this species difference could be due to the proposed transiently forming salt bridge between E299 and R324 in *Brienomyrus*. Based on this, we predicted that reverting E299 to the ancestral amino acid at that site (E299T) should produce a faster deactivation time constant (tau_{deact}) than the WT. When comparing tau_{deact} across channels it is important to adjust for differences in $V_{1/2}$. The $V_{1/2}$ of WT *Brienomyrus* Kv1.7a is ~10 mV more negative than the E299T mutant channel so that a proper comparison would "slide" the deactivation curve for the WT +10 mV along the x axis. As predicted, E299T tau_{deact} (-50 mV) is significantly faster than WT (-40 mV) ($p<0.038$ one way t-test). Also consistent with our MD simulations, altering this site in *Gymnarchus* did not affect tau_{deact} (Fig. 11).

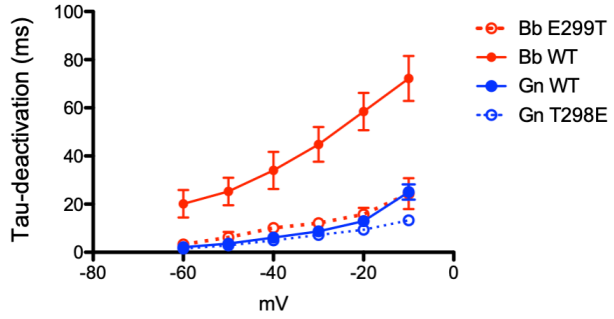

Figure 11—Neutralization of *Brienomyrus* E299 decreases deactivation time constant. Time constant (tau) of deactivation following different voltage clamp steps for *Gymnarchus* (Gn) and *Brienomyrus* (Bb) Kv1.7a wild type (WT) channels and with position 299 neutralized (E299T) in *Brienomyrus* or with a negatively charged glutamate (T298E) substituted in *Gymnarchus*.

DISCUSSION

The S3-S4 Linker Negative Patch adds to Surface Charge

African mormyrid fish evolved a patch of negatively charged amino acids in the S3-S4 linker in the Kv1.7a channel that is expressed in their electric organs; this patch enhances the voltage-dependence of the channel, shortening the electric organ action potential and resulting in a brief EOD. We hypothesized that this patch adds negative surface charge to the extracellular side of the channel (4). In the current paper, we tested this hypothesis further. First, we used Sr^{2+} to screen the negative charges. That the G-V

curve and $V_{1/2}$ of Kv1.7a from *Gymnarchus* were largely unaffected by the addition of 50 mM $SrCl_2$ was expected as its S3-S4 linker is composed of neutral amino acids. Our previous work showed that placing the *Brienomyrus* negative patch into the *Gymnarchus* S3-S4 linker shifted the G-V curve leftward and moved $V_{1/2}$ to more hyperpolarized values. We found that Sr^{2+} moved these parameters back to baseline values as if all the negative charge was neutralized. The Kv1.7a of *Brienomyrus* behaved in a complementary manner. Addition of $SrCl_2$ shifted the G-V curve rightward and moved $V_{1/2}$ to more positive values where these overlapped with the values of Kv1.7a with the negative patch replaced with *Gymnarchus*' neutral amino acids. However, the addition of $SrCl_2$ to the chimeric channel moved the G-V curve further rightward and $V_{1/2}$ to even more depolarized values. Future studies are needed to explain the "excess" effect of Sr^{2+} on the *Brienomyrus* EEEE>SPT chimera.

The S3-S4 linker has other charged amino acids beside the negative patch (Fig. 1). However, alteration of these to opposite charges in a previous study had little to no effect on the G-V curve suggesting that they are electrically distant from the voltage sensor (4). In agreement with (17) we observed that charge switching of AAs at other sites in the channel (e.g.—S1-S2 extracellular loop) shifted the G-V curve rightward. However, the results of the Sr^{2+} experiments suggest that these other regions minimally contribute to surface charge compared to the negative patch.

Second, to give more insight into the role of each glutamate, we replaced three of the glutamates with glycine and left a single glutamate in positions 1-4. This analysis suggested that each glutamate equally influences $V_{1/2}$ and that none of the AAs in the negative patch are too far to exert an electrical impact. The observation that each of the glutamates carries equal weight does not reconcile with the differences we found in the effects of paired glutamates in which the pairs of glutamates at positions 2 and 4 were consistently more effective in shifting $V_{1/2}$ than those in positions 1 and 3. The most likely reason is that the S3-S4 linker with paired glutamates is structurally more like the native S3-S4 helix. However, these differences, while significant, are not major.

Third, the G-V curves of currents from channels with different numbers of glutamates have similar slopes suggesting that the glutamates in the S3-S4 linker do not directly interact with the voltage sensor but, rather, simply add surface charge.

Fourth, our MD simulations showed that the negative patch lies at the membrane-fluid interface and interacts with cations and positive head groups of membrane lipids and not amino acids in the channel protein.

Our results are consistent with (19) who experimentally varied the length and AA composition of the S3-S4 loop and found that glutamates were more effective than glycines or serines in shifting $V_{1/2}$ to hyperpolarized potentials. Similarly, (39) found that the substitution of glutamates into the S3-S4 linker of *Shaker* left-shifted the G-V curve. Other studies have shown that evolutionary changes in AA sequence may influence extracellular or intracellular surface charge and shift membrane potential depending on the polarity of charge and its position in an extra- or intracellular loop (e.g.--Kv channel of squid axon: (40); Cav1.3 of skate: (41)).

Further Insights from MD Simulations

MD simulations of the *Brienomyrus* Kv1.7a show that in the resting state, the S3-S4 loop is helical and a continuation of the S4 helix, but that this helix unfolds in the active state. Interestingly, It has been suggested that this loop may be helical in some Kv channels (42). A possible, though speculative, mechanistic role for this helix might be related to its stiffness: in the resting state upwards motion of S4 may be partially hindered by this structural element; unfolding of the helix would then result in an increased mobility of S4 and thus a prompt response to depolarization. One advantage of the helical structure is that it results in a remarkable spatial proximity of the glutamates, which form a compact cluster at the top of S4. It is important to emphasize that, among all amino acids, glutamates have a reasonably high propensity to form helices (43).

***Brienomyrus* E299 Interacts with a Gating Charge**

Common to site 299/298 in the S3b of both species is that hydrophobic AAs make the channel more voltage-dependent while positively charged AA at this site decrease voltage-dependency. These observations are in keeping with the *Drosophila shaker* channel in which insertions of a string of identical hydrophobic AAs in S3b lowered voltage-dependency whereas hydrophilic AAs raised it (36). The second observation is also consistent with this site being exposed to the extracellular fluid and therefore additionally contributing to surface charge.

In the *Gymnarchus* Kv1.7a S3b, polar AAs substitute for threonine at site 298 with minimal effects on $V_{1/2}$. On the other hand, the *Brienomyrus* channel is sensitive to substitutions even of polar hydrophilic AAs, including negatively charged aspartate. The species difference is probably because T298 of *Gymnarchus* is not positioned to interact with the gating charges in S4 whereas E299 of *Brienomyrus* faces the membrane at rest (where it adds to surface charge along with the negative patch in the S3-S4 linker) but pivots to face the second gating charge (R234) in the open state where they are predicted to be close enough (1.5 Å) to form a salt bridge (44) and stabilize the open state. It may be that even aspartate cannot substitute for glutamate in the *Brienomyrus* S3b if aspartate is not close enough to R234 to form a salt bridge. This hypothesis can be tested further in the future by neutralizing R2 which we predict would decrease the time in the open state.

It is likely that the species-specific difference in positioning of site 299/298 derives from other amino acid substitutions in the *Brienomyrus* S3b. The S3b of the *Gymnarchus* Kv1.7a differs from human Kv1.7 in only 1/11 positions and from *Drosophila shaker* in only 4/11 positions. Remarkably, despite the relative phylogenetic closeness of these two species, the S3b of *Brienomyrus* and *Gymnarchus* differ in 8/11 positions. Further, the S3b of *Brienomyrus* differs from that of human in 9/11 positions and *Drosophila* in 8/11 positions). We propose that these other amino acid substitutions in the S3b are responsible for helping to position E299 toward the S4. Alternatively, the formation of the salt bridge alone might be sufficient to stabilize the interaction between S4 and S3b. In that case, it is not clear what function the other amino acid substitutions in the S3b might serve.

From an evolutionary point of view, given the conservation of a threonine at site 299 (with occasional independent substitutions to alanine) among animal *shaker* subfamily channels, it would seem unlikely that selection would favor altering this site from T>A>E when this does so little to alter $V_{1/2}$. The answer is probably that other amino acid substitutions in S3b preceded the final substitution to glutamate in an ancestral mormyrid or the T>A was a neutral substitution (which is not deleterious because it is observed in shark and mammals, Fig. 1) followed by the A>E which was then selected.

Historically, three amino acid sites have been designated as negative countercharges that interact with the gating charges of the S4 voltage sensor (45,46) although the role of two of these (*shaker* numbering = E293, D316) as salt-bridge forming countercharges has been questioned (47). We propose that a novel negative countercharge evolved in a mormyrid ancestor between E299—uniquely found in mormyrids--and R324 (or R2, the second gating charge). The evidence for this is that these two amino acids are poised a few Ångstroms of each other in open state simulations and that the rate of deactivation is sped up with a neutral polar substitution (threonine) at E299. Even a negatively charged aspartate at that site does not substitute for a glutamate.

Since a channel's voltage-sensitivity is influenced by the number of positive charges in the S4 and their interactions with negative countercharges, we wondered if the evolution of a novel countercharge affected the voltage-sensitivity of mormyrid Kv1.7a. We noted that reverting the mormyrid E299 to its ancestral T299 or other amino acids--excepting hydrophobic ones--did not

alter slope factor. Because E299 is at the uppermost end of S3b and our modeling predicts that S4 and S3b rotate toward each other during activation, E299 and R2 may only be close enough to interact once the voltage sensor is fully raised. Thus, their interaction impacts deactivation rather than activation as some AA substitutions are known to do (47,48).

Is the Novel S3b Countercharge Generalizable to Other Species or Channels?

Is the evolution of a negative amino acid in S3b and a gating charge that enhances voltage-dependency unique to the mormyrid Kv1.7a channel? While a negatively charged amino acid at the homologous position to E299 is not observed in bilateria, it occurs in a cnidarian Kv channel, shak5. Intriguingly, of the six shak channels in the sea anemone (*Nematostella vectensis*) shak5 is the most voltage-dependent ($V_{1/2}$ = -30 mV) (Jegla et al., 2012). A broader assessment of animal Kv channels (Kv2, Kv3, Kv4) shows that a negatively charged AA (glutamate in vertebrate Kv3, aspartate in the related invertebrate *shaw* channels), or uncharged polar AA occurs at this site in Kv2 (threonine in vertebrates or serine in invertebrate *shab* homologs) and Kv4 (glycine). Thus, while the identity of the AA at this site is not as universally conserved across all voltage-gated channels as are other key residues (e.g.--arginines in the S4 or negatively charged AAs in S2 and S3) (22), in the Kv family, we note primarily neutral or, less frequently negatively charged, AAs at this site. The occasional appearance of a negatively charged AA at this site in other *shaker* family channels raises the question as to whether they might also function as a negative countercharge.

Coevolution of T299E and S4 Voltage Sensor in Mormyrids

A striking feature of the S4 voltage sensor of Kv1.7a in mormyrids is that its first three amino acids (KIV) differ from those of the S4s of other *shaker* channels (RVI) (Fig. 1). We previously observed that reverting the mormyrid gating charge (K>R), the adjacent two hydrophobic amino acids (IV>VI), or all three (KIV>RVI), had no effect on $V_{1/2}$ or activation time constants, but profoundly sped up the tau_{deact} (WT = 20 ms; K>R =10 ms; IV>VI = 12 ms; KIV>RVI = 7 ms). It is a particular mystery why the highly conserved first gating charge is a lysine in mormyrid Kv1.7a. Lysine and arginine have equivalent charge, but arginine can form more salt bridges or hydrogen bonds with nearby amino acids than lysine (49,50). During deactivation the S4 transitions from a position of maximum height--the up state--*via* intermediate positions to its lowest position--the down state (51). If the usual first gating charge (R1) formed a salt bridge with the evolutionarily novel E299, S4 would be held in an intermediate state whereas if the salt bridge is with the second gating charge (R2) the S4 is held in the up state. The higher the S4 resides in the membrane, the more states it must pass through, and presumably the more time it would take, for it to return to the down state. Perhaps a lysine in the position of the first gating charge is less “competitive” with the R2 in binding with E299 thereby allowing the S4 to be held at its highest extent in the up state.

But why is a slow tau_{deact} important for mormyrid electrocytes, the single cells of the electric organ? The EO can be schematized as a battery with an internal resistance that passes current across an external load (the resistance of the water). That is, a voltage divider. For maximum voltage drop across the external load, the internal resistance of the EO should be small. We hypothesize that the slow deactivation of Kv1.7a channels aids in minimizing internal resistance by maintaining the Kv1.7a channels open during much of the discharge. Recordings from the mormyrid EO show that the internal resistance of the EO is low during the EOD (10,52,53). Additionally, maintaining a strongly hyperpolarized V_m may efficiently remove inactivation from the electrocyte’s Nav channels thereby allowing maximum Na^+ currents.

Conclusion

The potassium channel Kv1.7a, which is expressed in the electric organ of African weakly electric fish (mormyrids), activates at more hyperpolarized voltages than most Kv channels. Its enhanced voltage dependence and rapid activation help to generate a brief action potential (~0.2 ms) that shapes a brief electric organ discharge. Kv1.7a of mormyrids has several amino acid substitutions compared to the same channel in other species that do not express this channel in their electric organs. In this study, we examined the role of the "negative patch"—four consecutive negatively charged glutamates—in the S3-S4 linker and determined that it adds to the membrane surface charge. This facilitates channel activation at more hyperpolarized potentials than Kv1.7a in non-mormyrid species. Another unique feature of the mormyrid Kv1.7a is a glutamate at a site in the S3b helix that is occupied by neutral amino acids, usually threonine, in the Kv1.7 of most animals. We determined that a glutamate at this site acts as a negative countercharge to one of the positive gating charges in the S4 (R2) which biases the channel in the open state causing a prolonged deactivation. The enhanced voltage-dependence of this channel is imparted by these two complementary mechanisms.

Author contributions: HZ and VC designed the project; SI and JT constructed expression vectors, performed mutagenesis, and made recordings; VC and AS performed molecular dynamic simulations; all authors participated in writing the manuscript.

Declaration of interests: None of the authors have any interests to declare.

Acknowledgments: IS, JT, and HZ were supported by National Science Foundation grant 1856695 to HZ. VC was supported by the National Institute of General Medical Science of the National Institutes of Health under award number R01GM093290. This research includes calculations carried out on Temple University's HPC resources and thus was supported in part by the National Science Foundation through major research instrumentation grant number 1625061 and by the US Army Research Laboratory under contract number W911NF-16-2-0189. We thank the *Xenopus* facility at the Animal Care Center at the University of Texas and colleagues who helped with dissection and oocyte preparation. We thank Nicole Elmer for help with artwork.

BIBLIOGRAPHY

1. Sharmin, N., and W. J. Gallin. 2017. Intramolecular interactions that control voltage sensitivity in the jShak1 potassium channel from Polyorchis penicillatus. *J Exp Biol*. 220(Pt 3):469-477, doi: 10.1242/jeb.144089.
2. Jegla, T., and L. Salkoff. 1997. A novel subunit for shal K+ channels radically alters activation and inactivation. *J Neurosci*. 17(1):32-44, doi: 10.1523/jneurosci.17-01-00032.1997.
3. Shahidullah, M., and M. Covarrubias. 2003. The link between ion permeation and inactivation gating of Kv4 potassium channels. *Biophys J*. 84(2 Pt 1):928-941, doi: 10.1016/s0006-3495(03)74910-8.
4. Swapna, I., A. Ghezzi, J. M. York, M. R. Markham, D. B. Halling, Y. Lu, J. R. Gallant, and H. H. Zakon. 2018. Electrostatic Tuning of a Potassium Channel in Electric Fish. *Curr Biol*. 28(13):2094-2102 e2095, doi: 10.1016/j.cub.2018.05.012, https://www.ncbi.nlm.nih.gov/pubmed/29937349.
5. Kalman, K., A. Nguyen, J. Tseng-Crank, I. D. Dukes, G. Chandy, C. M. Hustad, N. G. Copeland, N. A. Jenkins, H. Mohrenweiser, B. Brandriff, M. Cahalan, G. A. Gutman, and K. G. Chandy. 1998. Genomic Organization, Chromosomal Localization, Tissue Distribution, and Biophysical Characterization of a Novel Mammalian *Shaker*-related Voltage-gated Potassium Channel, Kv1.7. *Journal of Biological Chemistry*. 273(10):5851-5857, doi: 10.1074/jbc.273.10.5851, https://doi.org/10.1074/jbc.273.10.5851.
6. Kashuba, V. I., S. M. Kvasha, A. I. Protopopov, R. Z. Gizatullin, A. V. Rynditch, C. Wahlestedt, W. W. Wasserman, and E. R. Zabarovsky. 2001. Initial isolation and analysis of the human Kv1.7 (KCNA7) gene, a member of the voltage-gated potassium channel gene family. *Gene*. 268(1):115-122, doi: https://doi.org/10.1016/S0378-1119(01)00423-1, https://www.sciencedirect.com/science/article/pii/S0378111901004231.
7. Hopkins, C. D. 1980. Evolution of Electric Communication Channels of Mormyrids. *Behav Ecol Sociobiol*. 7:1-13.
8. Sullivan, J. P., S. Lavoue, and C. D. Hopkins. 2000. Molecular systematics of the African electric fishes (Mormyroidea: teleostei) and a model for the evolution of their electric organs. *The Journal of experimental biology*. 203(Pt 4):665-683, http://jeb.biologists.org/cgi/pmidlookup?view=long&pmid=10648209.
9. Bass, A., and S. Volman. 1987. From behavior to membranes: Testosterone-induced changes in action potential duration in electric organs. *Proc. Natl. Acad. Sci. USA*. 84:9295-9298.
10. Bennett, M. V. L. 1971. Electric Organs. In Fish Physiology. W. S. Hoar, and D. J. Randall, editors. Academic Press, pp. 347-491.
11. Bezanilla, F. 2018. Gating currents. *Journal of General Physiology*. 150(7):911-932, doi: 10.1085/jgp.201812090, https://doi.org/10.1085/jgp.201812090.
12. Ledwell, J. L., and R. W. Aldrich. 1999. Mutations in the S4 region isolate the final voltage-dependent cooperative step in potassium channel activation. *J Gen Physiol*. 113(3):389-414, doi: 10.1085/jgp.113.3.389.

13. Smith-Maxwell, C. J., J. L. Ledwell, and R. W. Aldrich. 1998. Uncharged S4 residues and cooperativity in voltage-dependent potassium channel activation. *J Gen Physiol*. 111(3):421-439, doi: 10.1085/jgp.111.3.421.
14. Aggarwal, S. K., and R. MacKinnon. 1996. Contribution of the S4 segment to gating charge in the *Shaker* K^+ channel. *Neuron*. 16(6):1169-1177, doi: 10.1016/s0896-6273(00)80143-9.
15. Lopez, G. A., Y. N. Jan, and L. Y. Jan. 1991. Hydrophobic substitution mutations in the S4 sequence alter voltage-dependent gating in shaker K^+ channels. *Neuron*. 7(2):327-336, doi: 10.1016/0896-6273(91)90271-Z, https://doi.org/10.1016/0896-6273(91)90271-Z.
16. Elinder, F., and P. Århem. 1999. Role of Individual Surface Charges of Voltage-Gated K Channels. *Biophysical Journal*. 77(3):1358-1362, doi: https://doi.org/10.1016/S0006-3495(99)76984-5, https://www.sciencedirect.com/science/article/pii/S0006349599769845.
17. Elinder, F., M. Madeja, and P. Arhem. 1996. Surface Charges of K channels. Effects of strontium on five cloned channels expressed in Xenopus oocytes. *J Gen Physiol*. 108(4):325-332, doi: 10.1085/jgp.108.4.325.
18. Elinder, F., M. Madeja, H. Zeberg, and P. Århem. 2016. Extracellular Linkers Completely Transplant the Voltage Dependence from Kv1.2 Ion Channels to Kv2.1. *Biophysical Journal*. 111(8):1679-1691, doi: https://doi.org/10.1016/j.bpj.2016.08.043, https://www.sciencedirect.com/science/article/pii/S0006349516307676.
19. Sand, R., N. Sharmin, C. Morgan, and W. J. Gallin. 2013. Fine-tuning of Voltage Sensitivity of the Kv1.2 Potassium Channel by Interhelix Loop Dynamics. *Journal of Biological Chemistry*. 288(14):9686-9695.
20. Matthies, D., C. Bae, G. E. S. Toombes, T. Fox, A. Bartesaghi, S. Subramaniam, and K. J. Swartz. 2018. Single-particle cryo-EM structure of a voltage-activated potassium channel in lipid nanodiscs. *eLife*. 7:e37558, doi: 10.7554/eLife.37558, https://doi.org/10.7554/eLife.37558.
21. Wisedchaisri, G., L. Tonggu, E. McCord, T. M. Gamal El-Din, L. Wang, N. Zheng, and W. A. Catterall. 2019. Resting-State Structure and Gating Mechanism of a Voltage-Gated Sodium Channel. *Cell*. 178(4):993-1003.e1012, doi: 10.1016/j.cell.2019.06.031.
22. Palovcak, E., L. Delemotte, M. L. Klein, and V. Carnevale. 2014. Evolutionary imprint of activation: the design principles of VSDs. *J Gen Physiol*. 143(2):145-156, doi: 10.1085/jgp.201311103.
23. Waterhouse, A., M. Bertoni, S. Bienert, G. Studer, G. Tauriello, R. Gumienny, F. T. Heer, T. A P. de Beer, C. Rempfer, L. Bordoli, R. Lepore, and T. Schwede. 2018. SWISS-MODEL: homology modelling of protein structures and complexes. *Nucleic Acids Research*. 46(W1):W296-W303, doi: 10.1093/nar/gky427, https://doi.org/10.1093/nar/gky427.
24. Stein, A., and T. Kortemme. 2013. Improvements to Robotics-Inspired Conformational Sampling in Rosetta. *PLOS ONE*. 8(5):e63090, doi: 10.1371/journal.pone.0063090, https://doi.org/10.1371/journal.pone.0063090.
25. Barth, P., J. Schonbrun, and D. Baker. 2007. Toward high-resolution prediction and design of transmembrane helical protein structures. *Proc Natl Acad Sci U S A*. 104(40):15682-15687, doi: 10.1073/pnas.0702515104.

26. Wu, E. L., X. Cheng, S. Jo, H. Rui, K. C. Song, E. M. Dávila-Contreras, Y. Qi, J. Lee, V. Monje-Galvan, R. M. Venable, J. B. Klauda, and W. Im. 2014. CHARMM-GUI Membrane Builder toward realistic biological membrane simulations. *J Comput Chem*. 35(27):1997-2004, doi: 10.1002/jcc.23702.
27. Phillips, J. C., R. Braun, W. Wang, J. Gumbart, E. Tajkhorshid, E. Villa, C. Chipot, R. D. Skeel, L. Kalé, and K. Schulten. 2005. Scalable molecular dynamics with NAMD. *J Comput Chem*. 26(16):1781-1802, doi: 10.1002/jcc.20289.
28. Mackerell, A. D., Jr., M. Feig, and C. L. Brooks, 3rd. 2004. Extending the treatment of backbone energetics in protein force fields: limitations of gas-phase quantum mechanics in reproducing protein conformational distributions in molecular dynamics simulations. *J Comput Chem*. 25(11):1400-1415, doi: 10.1002/jcc.20065.
29. Essmann, U., L. Perera, M. L. Berkowitz, T. Darden, H. Lee, and L. G. Pedersen. 1995. A smooth particle mesh Ewald method. *The Journal of Chemical Physics*. 103(19):8577-8593, doi: 10.1063/1.470117, https://doi.org/10.1063/1.470117.
30. Frankenhaeuser, B., and A. L. Hodgkin. 1957. The action of calcium on the electrical properties of squid axons. *J Physiol*. 137(2):218-244, doi: 10.1113/jphysiol.1957.sp005808.
31. Hille, B., M. Woodhull, B. I. Shapiro, R. C. Thomas, and R. D. Keynes. 1997. Negative surface charge near sodium channels of nerve: divalent ions, monovalent ions, and pH. *Philosophical Transactions of the Royal Society of London. B, Biological Sciences*. 270(908):301-318, doi: 10.1098/rstb.1975.0011, https://doi.org/10.1098/rstb.1975.0011.
32. Broomand, A., F. Osterberg, T. Wardi, and F. Elinder. 2007. Electrostatic domino effect in the Shaker K channel turret. *Biophys J*. 93(7):2307-2314, doi: 10.1529/biophysj.107.104349.
33. Hoshi, T., and C. M. Armstrong. 2012. Initial steps in the opening of a Shaker potassium channel. *Proc Natl Acad Sci U S A*. 109(31):12800-12804, doi: 10.1073/pnas.1209665109.
34. Zhang, R. B., and A. S. Verkman. 1991. Water and urea permeability properties of Xenopus oocytes: expression of mRNA from toad urinary bladder. *American Journal of Physiology-Cell Physiology*. 260(1):C26-C34, doi: 10.1152/ajpcell.1991.260.1.C26, https://doi.org/10.1152/ajpcell.1991.260.1.C26.
35. Hui Li, H., A. D. Robertson, and J. H. Jensen. 2005. Very Fast Empirical Prediction and Interpretation of Protein pKa Values. *Proteins*. 61:704-721.
36. Xu, Y., Y. Ramu, H. G. Shin, J. Yamakaze, and Z. Lu. 2013. Energetic role of the paddle motif in voltage gating of Shaker K^+ channels. *Nat Struct Mol Biol*. 20(5):574-581, doi: 10.1038/nsmb.2535.
37. Delemotte, L., M. A. Kasimova, M. L. Klein, M. Tarek, and V. Carnevale. 2014. Free-energy landscape of ion-channel voltage-sensor–domain activation. *Proc Natl Acad Sci U S A*. 112(1):124-129.
38. Huang, G., Q. Wu, Z. Li, X. Jin, X. Huang, T. Wu, X. Pan, and N. Yan. 2022. Unwinding and spiral sliding of S4 and domain rotation of VSD during the electromechanical coupling in Nav1.7. *Proc Natl Acad Sci U S A*. 119(33).

39. Carvalho-de-Souza, J. L., and F. Bezanilla. 2018. Nonsensing residues in S3–S4 linker's C terminus affect the voltage sensor set point in K+ channels. *Journal of General Physiology*. 150(2):307-321, doi: 10.1085/jgp.201711882, https://doi.org/10.1085/jgp.201711882.
40. Perozo, E., and F. Bezanilla. 1991. Phosphorylation of K+ channels in the squid giant axon. A mechanistic analysis. *Journal of Bioenergetics and Biomembranes*. 23(4):599-613, doi: 10.1007/BF00785813, https://doi.org/10.1007/BF00785813.
41. Bellono, N. W., D. B. Leitch, and D. Julius. 2017. Molecular basis of ancestral vertebrate electroreception. *Nature*. 543(7645):391-396, doi: 10.1038/nature21401, https://doi.org/10.1038/nature21401.
42. Yang, Y. C., S. Lin, P. C. Chang, H. C. Lin, and C. C. Kuo. 2011. Functional extension of amino acid triads from the fourth transmembrane segment (S4) into its external linker in Shaker K^+ channels. *J Biol Chem*. 286(43):37503-37514, doi: 10.1074/jbc.M111.237792.
43. Pace, C. N., and J. M. Scholtz. 1998. A helix propensity scale based on experimental studies of peptides and proteins. *Biophys J*. 75(1):422-427, doi: 10.1016/s0006-3495(98)77529-0.
44. Kumar, S., and R. Nussinov. 2002. Close-range electrostatic interactions in proteins. *Chembiochem*. 3(7):604-617, doi: 10.1002/1439-7633(20020703)3:7<604::Aid-cbic604>3.0.Co;2-x.
45. Groome, J. R., and L. Bayless-Edwards. 2020. Roles for Countercharge in the Voltage Sensor Domain of Ion Channels. *Front Pharmacol*. 11:160, doi: 10.3389/fphar.2020.00160.
46. Seoh, S. A., D. Sigg, D. M. Papazian, and F. Bezanilla. 1996. Voltage-sensing residues in the S2 and S4 segments of the Shaker K+ channel. *Neuron*. 16(6):1159-1167, doi: 10.1016/s0896-6273(00)80142-7.
47. Pless, S. A., J. D. Galpin, A. P. Niciforovic, and C. A. Ahern. 2011. Contributions of counter-charge in a potassium channel voltage-sensor domain. *Nat Chem Biol*. 7(9):617-623, doi: 10.1038/nchembio.622.
48. Infield, D. T., E. E. L. Lee, J. D. Galpin, G. D. Galles, F. Bezanilla, and C. A. Ahern. 2018. Replacing voltage sensor arginines with citrulline provides mechanistic insight into charge versus shape. *J Gen Physiol*. 150(7):1017-1024, doi: 10.1085/jgp.201812075.
49. Armstrong, C. T., P. E. Mason, J. L. R. Anderson, and C. E. Dempsey. 2016. Arginine side chain interactions and the role of arginine as a gating charge carrier in voltage sensitive ion channels. *Scientific Reports*. 6(1):21759, doi: 10.1038/srep21759, https://doi.org/10.1038/srep21759.
50. Li, L., I. Vorobyov, and T. W. Allen. 2013. The Different Interactions of Lysine and Arginine Side Chains with Lipid Membranes. *The Journal of Physical Chemistry B*. 117(40):11906-11920, doi: 10.1021/jp405418y, https://doi.org/10.1021/jp405418y.
51. Delemotte, L., M. Tarek, M. L. Klein, C. Amaral, and W. Treptow. 2011. Intermediate states of the Kv1.2 voltage sensor from atomistic molecular dynamics simulations. *Proc Natl Acad Sci U S A*. 108(15):6109-6114, doi: 10.1073/pnas.1102724108.
52. Bell, C. C., J. Bradbury, and C. J. Russell. 1976. The electric organ of a mormyrid as a current and voltage source. *Journal of comparative physiology*. 110:65-88.

53. Bennett, M. V., and H. Grundfest. 1961. Studies on the morphology and electrophysiology of electric organs. III. Electrophysiology of electric organs in mormyrids. *Bioelectrogenesis*.113-135.